

Power-Peaking Factors in the McMaster Nuclear Reactor

Simon E. Day
McMaster Nuclear Reactor
McMaster University
1280 Main St. W., Hamilton
Ontario, Canada L8S 4K1
Email: dayse@mcmaster.ca

Abstract

A review and update of the Safety Analysis Report¹ is a current, ongoing project at the McMaster Nuclear Reactor (MNR). Using modern codes and techniques the reactor physics characteristics of the MNR core are being detailed. This paper describes the reactor physics analysis of power peaking in MNR using the code package WIMS-AECL/3DDT²⁻⁶. The results are to be used as input for analysis on thermalhydraulic safety margins.

MNR is a 2 MW_{th}, light-water-moderated, pool-type reactor, composed of rectangular parallelepiped plate fuel. At present MNR is in the process of switching from HEU (93%) to LEU (20%) fuel by systematically replacing spent HEU fuel assemblies with fresh LEU assemblies. As a result, there are currently 5 different types of fuel assemblies in the MNR core.

This paper describes the modelling of these fuel assembly types for power-peaking factor determination. Fuel assemblies were examined in both a fuel lattice and moderating environment and the effect of the absorber rod bank position was studied. The overall power-peaking factors were determined as products of local, radial and axial contributions.

It was determined that adjacent moderating material has a significant effect on local power peaking in a fuel assembly as does burnup, loading and geometry of the fuel assemblies. Overall power-peaking factors of 2.47 → 3.73 are typical for 18-plate fuel whereas a limiting overall power-peaking factor of 5.04 was found for 10-plate HEU fuel in a typical MNR core. These numbers are found to be more conservative than previously reported estimates^{7,8} but should not result in any new safety issues.⁹

1.0 Introduction

In a nuclear reactor core the power density varies both within a given fuel assembly and over the entire core. This is of concern in thermalhydraulic analysis when considering thermal safety margins for reactor operation. These margins include onset of nucleate boiling, flow instability, departure from nucleate boiling, onset of bulk boiling and fuel centerline melting temperatures.

A common approach to take into account the power density distribution is to identify the “hot spot” in the reactor core, which represents the “worst case” scenario for thermalhydraulics, and evaluate the core performance under this set of conditions. This situation is a “worst case” from the standpoint of the closest approach to thermal limitations.

The “hot spot” is determined by finding a set of peak-to-average power density ratios for the reactor core. These are called power-peaking factors (PPF's) and are defined below:

$$\text{Local PPF} \equiv \frac{\text{maximum power density in the hot assembly}}{\text{maximum XY-averaged power density in the hot assembly}}$$

$$\text{Axial PPF} \equiv \frac{\text{maximum XY-averaged power density in the hot assembly}}{\text{average power density in the hot assembly}}$$

$$\text{Radial PPF} \equiv \frac{\text{average power density in the hot assembly}}{\text{average power density in the core}}$$

The local and axial power-peaking factors take into account the power distributions over a given assembly whereas the radial power-peaking factor accounts for the power distribution throughout the different assemblies in the core.

The overall power-peaking factor is simply the product of the local, axial and radial factors for the hot assembly.

$$\begin{aligned} \text{Overall PPF} &\equiv \text{Local PPF} \times \text{Axial PPF} \times \text{Radial PPF} \\ &= \frac{\text{maximum power density in the core}}{\text{average power density in the core}} \end{aligned}$$

In this study we define power-peaking factors for each fuel assembly type in the MNR core.

This analysis was performed for the McMaster Nuclear Reactor (MNR). MNR is a 2 MW_{th}, light-water-moderated, pool-type reactor, fueled with rectangular parallelepiped plate fuel. At present MNR is in the process of switching from HEU (93%) to LEU (20%) fuel by systematically replacing spent HEU fuel assemblies with fresh LEU assemblies. As a result, there are currently 5 different types of fuel assembly in the MNR core.

If there was no regional dependence on the fission reactions then each geometrically identical fuel plate would produce the same power, *i.e.*, for a 16-fuel-plate assembly each fuel-plate would produce 1/16th of the power for the assembly. Similarly for the 10-plate fuel each plate would produce 1/10th of the power for the assembly. However, factors such as coolant gap thickness and location of moderator outside the fuel assembly will influence the local power peaking factors. Likewise, non-uniform burnup, location of irradiation sites, reflector positions, and fuel loading patterns will all influence the power distribution, both in a given assembly and across a given core.

There are two stages to this analysis. The first is on the level of the fine structure of a fuel assembly. This is performed with a transport theory code and yields the local power-peaking factors, which describe power peaking between the individual fuel plates. In this study we examined two specific fuel scenarios which are typical of MNR. The first is the case of a repeatable fuel lattice, or in other words, a fuel assembly surrounded by other fuel assemblies of similar properties. The second case is concerned with a fuel assembly bordering on a moderating material region.

The second stage of the analysis is performed using a diffusion theory code to model the core geometry, with cross section input from the appropriate transport theory models. From this the

global power density distribution can be determined and used to calculate both the axial and radial power-peaking factors. These describe the axial power peaking within an individual fuel assembly and the power peaking among the different fuel assemblies respectively. A series of recent MNR core configurations, including two LEU-substituted cores, are examined.

2.0 Previous Work

Previous power-peaking estimates for MNR were reported in References 7 & 8. These results were based on Cores 48A & 48B (physically assembled in May & August 1996 respectively) and some perturbations to these core configurations. Typical MNR HEU 18-plate fuel was examined near the Central Irradiation Site (CIF) located in core site 5C.

The local power-peaking results in References 7 & 8 appear to be based upon a comparison of power densities at different diffusion-solution mesh points and do not take into account any of the fine structure (*i.e.*, individual fuel plates) of the fuel assembly itself.

In this respect, this analysis not only provides an up-to-date and more complete estimate of power-peaking factors but also an improved methodology for such calculations.

3.0 Codes

3.1 Transport Theory Code

The transport theory code WIMS-AECL²⁻⁴ was used for this analysis. The version of WIMS-AECL and the cross-section library used are listed below:

- WIMS-AECL Release WL2-4Z 1996-01-03
- WIMS ENDF/B-V LIBRARY VERSION 1.4W

The library is based on the ENDF/B-V data file, and contains cross sections for 168 nuclides, including 30 fissile isotopes and 45 fission products, in 89 energy groups. The energy group structure is divided into 42 thermal groups, 23 resonance groups and 24 fast groups.

The WIMS-AECL code generates burnup-dependent cross sections for the different materials in the model as well as cell-averaged values. The geometry for plate fuel is limited to 1D-infinite slab. All WIMS-AECL cases were executed on the AECL-CRL VAX system.

3.2 Diffusion Theory Code

The 3DDT⁵ code is a 3-dimensional diffusion theory code. In this analysis the cross section input data is provided by WIMS-AECL in the form of random-access files. The front-end code MAPDDT⁶ was used to prepare input for 3DDT. The versions of MAPDDT and 3DDT used in this analysis are listed below:

- MAPDDT Release V1-1D_Beta LD= 1996-03-13
- 3DDT Release V1-1C LD= 1995-08-16

All MAPDDT/3DDT cases were executed on the AECL-CRL VAX system.

4.0 Cases

Since the MNR core can contain various types of fuel assemblies, [Table 1](#) is presented which summarizes some key properties for the different fuel types. For more information see Reference 10. Of note is the high per-plate U-235 loading and density in the fuel meat for the HEU 10-plate fuel and the comparison of the U-235 density in the 18-plate HEU and LEU fuel. Of course, other factors are important to remember when treating power peaking and they include the stage of burnup of the individual assemblies and their specific core positions. The fuel meat in the HEU assemblies is either UAl_x-Al or UO_3-Al while that in the LEU assemblies is U_3Si_2-Al .

4.1 Local Power-Peaking Cases

The various types of plate-fuel were examined in two types of environment. The first is a “fuel lattice” environment modeled using reflective boundary conditions for a simple fuel assembly model. Effectively this models the fuel assembly in a repeating lattice of identical fuel assemblies. This is a reasonable approximation to the environment for a fuel assembly surrounded by other fuel assemblies in the MNR core.

It should be noted that the “fuel lattice” cases are all part of MNR data sets that have been validated and documented in References 11 and 12. These models were used to provide cross-section input for the diffusion code cases.

The second type of environment involved modelling a fuel assembly adjacent to a moderating region typical of fuel assemblies adjacent to in-core irradiation sites, reflector assemblies or the core periphery. Light water, graphite and beryllium were all studied as the moderating material in the “moderating environment” analysis.

These models were constructed by simply adding a moderator region the size of one MNR core site (half of the site was explicitly modelled with a reflective outer boundary condition) beyond the outer region of the respective fuel model.

The control fuel models considered in the local power-peaking analysis were for the lower section of the control fuel (*i.e.*, without the guide insert) and did not contain any absorber materials.

It was considered desirable to examine the various fuel types at specific degrees of burnup, the same for each fuel type, corresponding to fresh fuel, 1%, 25% and 50% U-235 depletion.

4.2 Global Power-Peaking Cases

The solutions to a series of 3DDT core models were examined to estimate typical axial and radial power-peaking factors. The following cores were examined:

- 48A - (assembled May 1996)
- 48E - (assembled February 1997)
- 48K - (assembled January 1998)
- 48M - (assembled May 1998)
- 49A - (assembled January 1999)
- 49B - (assembled March 1999)
- 49C - (assembled May 1999)
- 49D - (assembled July 1999)
- 48A - LEU (225g U-235) Substituted
- 49A - LEU (225g U-235) Substituted

The 48 series cores and core 49A show recent variation in the irradiation sites in MNR whereas a comparison of the 49 series cores shows the gradual introduction of fresh LEU (225g U-235 loading) assemblies. Since at the time of the analysis only a few LEU 225g 18-plate fuel assemblies, and no LEU control fuel assemblies, had been introduced to the core, two LEU-substituted cases were included. For these cases all fuel assemblies were substituted with LEU 225g 18-plate fuel and all control fuel assemblies were substituted with LEU control assemblies, at the same exposure (MWd) as the actual assemblies in the core of interest.

Typically, in MNR the absorber rod position at criticality varies from roughly 20 cm inserted (67% withdrawn) for a Xenon-free beginning-of-life (BOL) core to almost fully withdrawn for a Xenon-equilibrium end-of-life (EOL) core. Operating limits state that the core must not be critical with the absorber rods less than 50% withdrawn. MNR has 5 highly absorbing Cd/In/Ag absorber rods and one stainless steel rod. The latter is used for fine adjustments of core multiplication. It is usual for the 5 Cd/In/Ag rods to move together and be positioned at the same insertion. The above cores were all analyzed with the rod bank in the fully withdrawn position.

The effect of the absorber rods on the axial power profiles was examined by studying core 49A with the rods at different insertion positions ranging from fully withdrawn to 50% withdrawn (30 cm insertion) in increments of 5 cm. A case with the stainless steel regulating rod at 50% withdrawn with the other absorber rods in the fully withdrawn position was also examined.

Since burnup tends to flatten the axial power distribution, the limiting case of axial power peaking, found in a fresh fuel assembly can be taken as a conservative estimate. In this analysis the axial burnup is taken to be uniform for all assemblies which will result in a similar axial power distribution to the fresh fuel case and is therefore a conservative approximation.

5.0 Methodology

The analysis can be divided into two main sections, one for the calculation of the local power-peaking factors and the other for the calculation of the axial and radial power-peaking factors.

A local power-peaking factor expresses the power density distribution over a specific fuel assembly. As diffusion theory analysis is not suitable for regions with strong absorption, it cannot be used for cell calculations, such as those required for the local-power peaking analysis, because of the presence of the highly absorbing fuel regions. The heterogeneous cell calculations must therefore be performed using a transport theory model. Diffusion theory is however valid at the level of reactor calculation with low absorption homogenized cell properties

and is used for these large geometries, such as the complete MNR core, because transport theory solutions become too expensive for systems of this scale.

As a result, the reactor physics calculation technique applied is to examine the fine geometry of a fuel assembly using a transport theory model and then form region-averaged cross sections for use in the diffusion theory model from which the axial and radial power peaking is examined.

It is clear that parameters dependent on the fine geometry detail will not be available in the diffusion theory solution as they have been “averaged” (homogenized) at an earlier stage in the analysis. In order to take into account the fine-geometry-dependent power-peaking details in a fuel assembly the power-density distribution from the transport solution is examined. It is assumed that the geometry, including the environment, used in the transport models is a good representation of the actual geometry. As long as the geometry and environment is a good approximation to the actual case, the power density distribution should also be realistic.

5.1 Methodology for the Local Power-Peaking Analysis

All fuel cell models were constructed using the 1-D infinite slab geometry approximation. An example of this geometry approximation is shown in [Figure 1](#). The entire fuel assembly was modeled in each case, making use of symmetry in the fuel assembly with a reflective centerline condition. The 1-D geometry is infinite in the two dimensions perpendicular to the thickness of the fuel plates. Peripheral material such as surrounding water and side-plates are placed beyond the outer fuel plate in the model. The placement of this “peripheral” material constitutes the approximation used in the geometry model.

Fuel burnup power ratings for the WIMS-AECL models were set at 60 kW/fuel-assembly and 35 kW/control-fuel-assembly which are representative values for average assemblies in the 2 MW_{th} MNR core. These power ratings were converted to MW/THE, as this is what the WIMS-AECL code uses.

Three sets of WIMS-AECL inputs were constructed for the local power-peaking analysis. The steps in the methodology are described below:

- (1) The various “fuel lattice” cases were executed with long burnup times with ASCII output from Chains 2 & 16 activated on the SUPPRESS card in the WIMS-AECL input file.
- (2) U-235 atom densities in the fuel meat were extracted from the ASCII output in (1). The relationships between U-235 depletion and days at full power, at the nominal power rating, were determined for each fuel type.
- (3) Using the relationships found in (2), a second set of “fuel lattice” cases for each fuel type were constructed with specific length burnup times corresponding to 1%, 25% and 50% U-235 depletion. These cases were executed with regional output for the binary (tape 16) file activated only for the final burnup step. Note: Steps (1) & (2) were performed to reduce the size of the output files. Otherwise the regional data on the binary output files from (1) could be analyzed and interpolated where necessary.
- (4) The regional power densities per fuel plate were calculated from the output from (3). From this, local power-peaking factors for the fuel lattice cases were determined.
- (5) Material atom densities, from the binary output from (3), were used to construct the “moderating environment” cases for each fuel type at the previously mentioned burnup stages. These models were constructed by simply adding a water, or homogenized

graphite or beryllium reflector assembly region, the size of one MNR core site (half of the site was explicitly modeled with a reflective outer boundary condition) beyond the last slab region in the fuel lattice models.

- (6) The output from (5) was analyzed as in (4) to determine the local power-peaking factors for the moderating environment cases.

WIMS-AECL does not provide regional fission cross sections in its binary output file. However, assuming that the neutrons per fission (ν) in each fuel region is identical, the ratio of fission source rates should be the same as the ratio of fission rates in the geometry. Fresh fuel is found to be the limiting case and since the initial fresh fuel composition is the same for each fuel region this should be a good approximation. For the U-235 depleted cases this approximation is thought to be conservative since $\nu_{\text{Pu-239}} > \nu_{\text{U-235}}$, and is expected to be worse for LEU fuel due to more Pu-239 production. However, the effect is expected to be small, as Pu-239 buildup is relatively minor in MNR fuel.¹³

5.2 Methodology for the Axial & Radial Power-Peaking Analysis

For the axial and radial power-peaking factors the following steps were required for the analysis:

- (1) Diffusion theory solutions were obtained for the various cores under consideration.
- (2) The total fuel volume and average core power density were determined for each core under consideration.
- (3) For each fuel assembly the peak axial power density was compared to the average power density for that assembly.
- (4) For each fuel assembly the average power density was determined and the ratios with the average core power density were found.
- (5) The axial and radial power-peaking factors for the core and the specific fuel types were identified.

It should be noted that the power densities for individual fuel assemblies were always averaged radially over the assembly x-y mesh for the axial and radial analysis. Local variations were taken into account in the local power-peaking analysis

6.0 Results

6.1 Local Power Density Distribution Analysis

The local power-peaking factor is defined as the maximum-peak to maximum-XY-averaged power density in the hot assembly. A schematic of the local power density distribution for a plate fuel assembly is shown in [Figure 2](#). In this analysis we assume that the local power-peaking factor is axially uniform over an assembly.

It should be noted that the results for the HEU 18-plate MNR UAl_x-Al and Cintichem UO₃-Al fuel were almost identical so only the UO₃-Al results are included in this report. Similarly, only the HEU UO₃-Al control fuel results are presented.

In this study we examined two specific fuel scenarios which are typical of MNR. The first is the case of a repeatable fuel lattice, or in other words, a fuel assembly surrounded by other fuel assemblies of similar properties. These results are summarized in Section 6.1.1. The second case is concerned with a fuel assembly bordering on a moderating material region. These results are summarized in Section 6.1.2.

6.1.1 Fuel Lattice Environment

The local power-peaking factors for the different fuel types in a repeatable fuel lattice environment are shown in [Table 2](#) for each fuel type and each burnup. It can clearly be seen that local power-peaking factors are dependent not only on fuel type but also on fuel burnup. The similar-geometry 18-plate fuel types all show similar power-peaking factors with slightly higher values for the LEU versions. This is probably due to the increased U-235 loading in the LEU fuel (initially 284g and 225g of U-235 for the two types of LEU fuel compared to 196g of U-235 for the HEU fuel).

Fresh or slightly burnt (1% U-235 depletion) fuel shows the largest local power peaking over the geometry, with peaking diminishing as the fuel burnup increases (depleting U-235 re-balances power distribution).

The power peaking in the outer fuel plates is due to the more thermal spectrum as a result of the presence of more moderating material near the outer fuel plates relative to that near the inner fuel plates. This effect is most pronounced for the 18-plate fuel assemblies. In addition to the fact that the 18-plate fuel assemblies have smaller coolant channels between fuel plates than the 10-plate fuel assemblies, the 18-plate fuel assemblies only contain 16 fueled plates, as the outer plates are solid aluminum “dummy” plates. This accounts for a more moderating environment for the outer fuel plates relative to the inner fuel plates than in the 10-plate fuel assemblies.

For the cases of fresh and 1% U-235 depleted 18-plate fuel types, local power-peaking factors up to 1.22 to 1.29 are noted in the outer fuel plates. For a mid-burnup element of this type the maximum local power-peaking factors are on the order of 1.13 to 1.20 and the maximum values drop off to less than 1.10 for 50%-burnt fuel. The HEU 10-plate fuel shows much less local power peaking with maximum values of 1.05 for the outer plates in fresh and 1% U-235 depleted fuel, becoming smaller as fuel burnup increases.

It should also be noted that the results for the 18-plate and 10-plate fuel types are conservative. This conservatism is a result of the modelling limitations for this type of fuel geometry. Since we approximate the plate geometry by a 1-D infinite slab model, all peripheral moderating material is placed on the outer edge of the model (near the outermost fuel plate – see [Figure 1](#)). As a result, the moderation for the outer fuel plate is somewhat over-predicted, directly affecting the local power-peaking factors.

The control fuel assembly results show a different power-density distribution as compared to the 18-plate and 10-plate fuel assemblies with power peaking near the middle of the assembly rather than near the outer edges. This is due to the presence of the water-filled control slot between fuel plates 5 and 6, where the control rod is inserted. When the rod is withdrawn the slot is filled with pool water. The water in the control slot provides extra moderation for the surrounding plates and results in a more thermal spectrum and therefore a higher fission rate and power density.

The two types of control fuel show very similar power-peaking results. This result is expected as the U-235 loadings are very similar (initially 110 g and 112 g of U-235 for HEU and LEU respectively). As in the case of the 18-plate and 10-plate fuel assemblies the control assemblies show local power-peaking factors that are very burnup dependent. Plates 5 and 6 in the control assemblies show local power-peaking factors of 1.14 to 1.17 in fresh and 1% burnt fuel. These values drop to roughly 1.10 and 1.03 for 25% and 50% U-235 depleted fuel.

The 1-D infinite slab approximation was also used for the control fuel models. Again, the effect of using this model is that slightly more moderating material is placed beyond the last fuel plate. However, unlike the standard fuel cases, in the case of the control fuel the inner plates show the highest power peaking. This may mean that our results slightly underestimate the local power-peaking factors for the central plates. Since the moderating material placed on the outer edge of the model is small in volume compared to the water in the central control slot ($\sim 1/8^{\text{th}}$), the underestimation is expected to be minor.

6.1.2 Moderating Environment

The location of moderating material is shown to be important to the local power-peaking factors in Section 6.2.1. The analysis was therefore extended to include fuel assemblies adjacent to moderating material regions the size of an entire MNR core site. This scenario exists in MNR for fuel assemblies near in-core irradiation sites and on the outer edge of the core. Results for the different fuel types are summarized in [Table 2](#) for light water, graphite reflector and beryllium reflector environments respectively.

As expected, when an 18-plate or 10-plate fuel assembly is adjacent to a water or reflector site in MNR, *i.e.*, there is a core site containing moderator beyond the outer fuel plate, the local power peaking is enhanced.

It was found that for 18-plate and 10-plate fuel assemblies all three moderating materials show similar local power-peaking factors. The light water cases show slightly larger local power-peaking factors than the graphite cases, which, in turn, show larger local power-peaking factors than the beryllium cases.

For the 18-plate fuel (both HEU and LEU), adjacent to a light water environment, the local power peaking for the fresh, 1% and 25% U-235 depleted cases is almost doubled when compared to the fuel lattice environment results. The most extreme case being for the LEU fuel with 284g U-235 loading, which shows local power-peaking of 1.52 for fresh and 1% burnup fuel. The LEU fuel with 225g U-235 loading per assembly shows a maximum local power-peaking factor of 1.45 in the outer fuel plate for 1% burnt fuel adjacent to the light water environment.

The 10-plate HEU fuel, which shows little in the way of local power peaking in a repeated fuel lattice environment, shows considerably higher local power-peaking factors when adjacent to a water, graphite or beryllium environment. This is not surprising as the environments for the outer and inner fuel plates are similar in the former case whereas they are quite different in the latter case.

For the control fuel assemblies, the moderating environment was placed beyond the 9th fuel plate in the assembly. The power peaking in the control assemblies is not as extreme as in the regular fuel assemblies in either the repeated fuel lattice or the moderating environment. However, unlike the regular fuel cases where the local power peaking is enhanced by the presence of the moderating environment, the local power-peaking factors are not significantly increased for the control assemblies. In fact, only the graphite cases show an increase in local power-peaking factors and it is very small.

All three moderating environment cases show a rebalancing of the power distribution towards the 9th fuel plate. The reason is that now the outer fuel plates, not just the inner plates adjacent to the control slot, are exposed to a more thermal flux environment. The result is that the power density is more uniform over the control assembly.

6.2 Global Power Density Distribution Analysis

The global power density distribution can be used to determine both the axial and radial power-peaking factors. These describe the axial power peaking within an individual fuel assembly and the power peaking among the different fuel assemblies in the core respectively. Power peaking within the plate-to-plate structure of an individual assembly is accounted for by the local power-peaking factors (see Section 6.1).

The axial and radial power peaking results are given in Sections 6.2.1 and 6.2.2 respectively.

6.2.1 Axial Power-Peaking Factors

The axial power-peaking factor is defined as the peak-to-average XY-averaged power density ratio for a given fuel assembly. A schematic of the axial power density distribution for a typical fuel assembly is shown in [Figure 3](#).

As a rough estimate one can examine the value calculated from one-speed diffusion theory. Assuming uniform axial fuel loading, the flux profile for a bare rectangular parallelepiped core, is given by a cosine distribution, peaking at the core centerline¹⁴:

$$\cos\left(\frac{\pi x}{\tilde{a}}\right)\cos\left(\frac{\pi y}{\tilde{b}}\right)\cos\left(\frac{\pi z}{\tilde{c}}\right)$$

Where \tilde{a} , \tilde{b} and \tilde{c} are the extrapolated x, y and z dimensions of the core. Assuming that the recoverable energy per fission and the one-speed fission cross section are all axially constant and the extrapolated height of the core is approximately equal to the physical height we find the axial power-peaking factor to be:

$$Axial\ PPF = \frac{\cos\left(\frac{\pi z}{\tilde{c}}\right)\Big|_{\max}}{\frac{1}{c} \int_{-c/2}^{c/2} \cos\left(\frac{\pi z}{\tilde{c}}\right) dz} \approx \frac{\pi}{2} \approx 1.57$$

When the analysis is made more realistic it is seen that this value is conservative. Specifically, the presence of an axial reflector, which is the case in MNR with light water both above and below the core, will serve to flatten the axial power density distribution and therefore reduce the axial power-peaking factor. In addition to this, as the fuel burnup increases the axial power density distribution is flattened since the fuel near the centerline burns at a higher rate than that near the core edges.

In our simulations of the MNR core, one of the approximations is the assumption of axially averaged burnup. For the reason stated above this should be a conservative estimate as far as axial power peaking is concerned.

From our examination of the various MNR cores listed in Section 4.2 for the cases where the absorber rods are in the fully withdrawn position, the typical limiting axial power-peaking factor for our simulation cases is 1.32. This is typical of all types of fuel and all core sites.

In order to address the effect of the absorber rods on the axial power distribution Core 49A was examined with the absorber rod bank at different degrees of insertion, ranging from fully withdrawn to 50% withdrawn (30 cm insertion).

It can be seen by examining the thermal flux depression (at constant power) due to the absorber rods, that although the flux depression inside the control fuel site is most pronounced there is still an overall thermal flux depression, on the order of 10-30%, in the axial zone where the absorbers are located.

Not surprisingly, it was found that the axial power peaking was increased the most in the control fuel assemblies due to the presence of the absorber. The rest of the fuel assemblies can be classified as either adjacent or diagonally adjacent to the control sites.

Limiting control fuel, adjacent and diagonally adjacent fuel axial power peaking values are given in [Table 3](#) for Core 49A with the absorber rods at various degrees of insertion. Clearly, the more inserted the rod bank the higher the axial power-peaking factors. The power density profiles for various Cd/In/Ag absorber rod insertions are shown in [Figure 4](#) for a control fuel assembly. This represents the limiting case for axial power peaking. Similar results were found for the adjacent and diagonally adjacent fuel assemblies and for the stainless steel absorber rod.

Comparisons of the control fuel with the adjacent and diagonally adjacent fuel assemblies for the absorber rods in the fully withdrawn and 50% withdrawn positions are shown in [Figure 5](#). Of note is that for the case where the absorber rods are in the fully withdrawn position all the fuel types showed almost identical axial power density profiles. This is expected since all diffusion models used in this analysis assumed uniform axial burnup.

Since MNR operating limits and conditions specify that, for a critical core, the absorber rods must be at least 50% withdrawn, the 50% withdrawn axial power-peaking factors were taken as the limiting conservative values. The control fuel assembly value was found to be 1.63 and the adjacent fuel assembly value was found to be 1.53. The adjacent fuel assembly value is applicable to both the 18-plate and 10-plate fuel types. These values should be representative of the various cores configurations.

Of further note is the fact that the actual location of the axial power density peak is not of paramount importance in MNR. The thermal margin does not change significantly down an

assembly. In addition to this, due to the low pressure, low flow characteristics of the facility the first critical thermalhydraulic event is found to be flow blockage, due to bubble formation.¹⁵ Once flow is stopped, similar thermalhydraulic conditions exist over the axial length of the assembly.

6.2.2 Radial Power-Peaking Factors

The radial power-peaking factor is defined as the average hot-assembly to core-average power density. A schematic of the radial power density distribution for a typical core is shown in [Figure 6](#). In our analysis we determined this value for each of the different types of fuel elements used in the MNR core.

The core-averaged power density is defined simply as the total core power divided by the total fuel volume in the core. The average power density values, as well as the total fuel volume and total U-235 loading for each core, for the various MNR cores are listed in [Table 4](#). The maximum radial power-peaking factors for each type of fuel assembly are listed in [Table 5](#) for each core configuration.

One factor that the reader should remain aware of is that the different fuel assembly types are not randomly placed throughout the MNR core and therefore the simulation values presented in this report do not represent a random fuel loading pattern but rather a realistic MNR fuel loading pattern.

For example, the two LEU 284g U-235 assemblies have not been, and are not planned to be, moved from their peripheral core sites (6A and 4F). As a result, the values for their radial power-peaking factors are low, as expected for these positions on the edge of the core. If, for example, they were moved into higher flux positions the radial power peaking factors would be expected to be similar to those of the HEU and LEU 225g U-235 18-plate fuel assemblies, which actually occupy these sites.

It should be noted that the position of the absorber rod bank affects the radial power-peaking factors. This can be seen in [Table 5](#) by comparing the results for Core 49A for different absorber rod insertions. The effect is significant in the control fuel assemblies but is quite small for the remainder of the fuel assemblies.

6.3 Overall Power-Peaking Factors

The overall power-peaking factor is defined as the product of the local, axial, and radial power-peaking factors for the hot-assembly. In this way the power distribution within the hot-assembly, both in the x-y plane and axially, is coupled with the radial power distribution of the core.

The limiting cases for the various fuel types are listed in [Table 6](#) and can be used in Safety Analysis related work in conjunction with core-averaged power density values. It is clear from [Table 6](#) that the HEU 10-plate fuel shows the largest overall power-peaking characteristics of all of the MNR fuel types (limiting overall power-peaking factor of 5.04) and therefore the highest power densities will be associated with this type of fuel. However, the 10-plate fuel assemblies also possess significantly larger coolant channels between fuel plates (0.644 cm as compared to

0.300 cm for the 18-plate assemblies) and thus the temperature effect of the higher power peaking should be somewhat reduced.

Of course, the relevant power-peaking factor, or combinations of factors, should be chosen to suit the subsequent thermalhydraulic analysis. For example, while the overall power-peaking factor is appropriate for a point model, only the local and radial power-peaking factors are required in a full-length channel analysis as the axial dimension is modelled explicitly, using an axial power density distribution.

For example, for a CATHENA¹⁶ model of MNR fuel, the required input is a power rating for a fictitious “hot assembly” and an axial power density shape. This hot assembly is defined as a fuel assembly consisting of fuel plates, which have power densities each equivalent to the “hot plate” identified above from the local and radial power-peaking factors. Power ratings for these fictitious hot assemblies are summarized in [Table 7](#). These values are based on the average power density for Core 49A, which was the maximum for all the cores used in this study.

The above mentioned data must be used in conjunction with the proper axial power density distribution. Representative examples of this are shown in [Figure 5](#) for the axially uniform burnup models used in this analysis.

7.0 Conclusions

The limiting power-peaking case appears to be a fresh HEU 10-plate fuel assembly next to a water environment such as the CIF (central irradiation facility) and adjacent to a control fuel assembly with the absorber rods in the 50% withdrawn position. This fuel type, in this environment, at this burnup shows a maximum overall power-peaking factor of 5.04 (the second highest overall power-peaking factor, 3.73, is for fresh LEU 225g U-235 18-plate fuel). This is much higher than the other fuel types and is due to the high per-plate U-235 loading and the larger coolant gaps between plates in the 10-plate HEU fuel assembly. These two factors result in higher fission rate densities for the 10-plate fuel.

It was also found that the positions of the absorber rods significantly affect the axial power density distributions. The axial power-peaking factors increase from roughly 1.32 for the cases where the absorber rods are located in the fully withdrawn position, to on the order of 1.53 → 1.63 for the cases where the absorber rods are located in a 50% withdrawn position. The axial power-peaking factors are conservative due to the approximation of uniform axial burnup used in the models used for this analysis.

These more conservative power-peaking factors do not result in any new safety issues for MNR as preliminary simulation results show that the temperatures are still below the thermalhydraulic limits.⁹

Acknowledgments

The author would like to thank Frank Saunders, Reactor Manager at the McMaster Nuclear Reactor for authorizing and funding this work as well as Wm. J. Garland of McMaster University and J. V. Donnelly of AECL for providing their helpful comments.

References

1. McMaster Nuclear Reactor Safety Report, McMaster University, Hamilton, Ontario, January 1972.
2. J. R. Askew, F. J. Fayers, P. B. Kemshell, "A General Description of the Lattice Code WIMS", *J. Brit. Nucl. Eng. Soc.*, v 5, pp. 564-585, 1966.
3. ORNL RSICC Computer Code Collection Documentation, "WIMSD4: Winfrith Improved Multigroup Scheme Code System", CCC-576 WIMS-D4, December 1990, revised October 1991.
4. J. Griffiths, "WIMS-AECL Users Manual", AECL RC-1176, COG-94-52, March 1994.
5. J. C. Vigil, "3DDT, A Three-Dimensional Multigroup Diffusion-Burnup Program", LA-4396, UC-32 Mathematics and Computers, TID-4500, September 1970, Argonne Code Center Abstract 463.
6. J. V. Donnelly, R. X. Slogoski, "User's Guide to MAPDDT", AECL, SAB-TN-126, SAB-011.004, January 21, 1988.
7. H. S. Al-Basha, "Reactor Physics Calculations for Conversion of McMaster Nuclear Reactor from Use of HEU to LEU Fuel", 19th Annual Conference of the Canadian Nuclear Society, Toronto, Ontario, October 18-21, 1998.
8. H. S. Al-Basha, "Reactor Physics Simulation of the MNR HEU Core", MNR Technical Report 97-05, Revision 1, July 15, 1997.
9. Personal communication with M. P. Butler, MNR Chief Reactor Supervisor (S. E. Day), March 2000.
10. S. E. Day, "MNR Core Component Technical Specifications", MNR Technical Report 1998-01, Rev. 2, April 21, 1999.
11. S. E. Day, "Core 49A Simulation – Validation of the NOV98 Data Set & Core Models", MNR Technical Report 1999-03.
12. S. E. Day, "MNR Flux Wire Irradiation Simulation – Validation of the APR99 Data Set & Core Models", MNR Technical Report, in progress.
13. M. P. Butler, "Comparison of Fission Product Inventories in MNR HEU and LEU Fuel Assemblies", MNR Technical Report 1998-04, July 3, 1998.
14. J. J. Duderstadt, L. J. Hamilton, *Nuclear Reactor Analysis*, John Wiley & Sons, Inc., 1976.
15. Wm. J. Garland, "Heat Transfer Limits for the McMaster Nuclear Reactor", MNR Technical Report 1999-01, February 17, 1999.
16. CAT-95, "CATHENA MOD-3.5 / Rev. 0, Theoretical Manual", Atomic Energy of Canada Limited, ed. B. N. Hanna, RC-982-3, 1995.

Table 1: MNR Fuel Assembly Properties

Fuel Type	Number of Fuel Plates per Assembly	Enrichment (% U-235)	Initial U-235 Nominal Loading (g/assembly)	Initial U-235 Density in Fuel Meat (g/cc)	Average Coolant Gap Thickness (cm)
HEU 18-Plate	16	93	196	0.643	0.300
HEU 10-Plate	10	93	160	0.839	0.644
LEU 225g 18-Plate	16	20	225	0.738	0.300
LEU 284g 18-Plate	16	20	284	0.931	0.300
HEU Control	9	93	110	0.643	0.300
LEU Control	9	20	112	0.656	0.300

Table 2: Local Power-Peaking Factors

Fuel Lattice Environment				
Fuel Type	Burnup (% U-235 Depletion)			
	Fresh	1%	25%	50%
HEU 18-plate	1.22	1.22	1.13	1.02
HEU 10-plate	1.05	1.05	1.03	1.00
LEU 225g 18-plate	1.25	1.25	1.17	1.06
LEU 284g 18-plate	1.29	1.29	1.20	1.08
HEU Control	1.17	1.17	1.10	1.02
LEU Control	1.17	1.17	1.11	1.03
Light Water Moderating Environment				
Fuel Type	Burnup (% U-235 Depletion)			
	Fresh	1%	25%	50%
HEU 18-plate	1.39	1.39	1.26	1.11
HEU 10-plate	1.22	1.23	1.17	1.10
LEU 225g 18-plate	1.44	1.45	1.32	1.18
LEU 284g 18-plate	1.52	1.52	1.39	1.22
HEU Control	1.14	1.14	1.10	1.07
LEU Control	1.14	1.14	1.11	1.09
Graphite Moderating Environment				
Fuel Type	Burnup (% U-235 Depletion)			
	Fresh	1%	25%	50%
HEU 18-plate	1.38	1.38	1.26	1.11
HEU 10-plate	1.21	1.21	1.17	1.10
LEU 225g 18-plate	1.43	1.43	1.31	1.17
LEU 284g 18-plate	1.50	1.50	1.37	1.21
HEU Control	1.18	1.18	1.14	1.12
LEU Control	1.18	1.18	1.16	1.14
Beryllium Moderating Environment				
Fuel Type	Burnup (% U-235 Depletion)			
	Fresh	1%	25%	50%
HEU 18-plate	1.32	1.33	1.21	1.06
HEU 10-plate	1.16	1.16	1.12	1.05
LEU 225g 18-plate	1.37	1.38	1.26	1.13
LEU 284g 18-plate	1.44	1.45	1.32	1.16
HEU Control	1.14	1.14	1.09	1.03
LEU Control	1.14	1.14	1.09	1.04

Table 3: Axial Power Peaking Factors for Various Absorber Rod Bank Insertions (Core 49A)

Limiting Fuel Assembly	Absorber Rod Bank Insertion						
	FWD	5 cm	10 cm	15 cm	20 cm	25 cm	30 cm
Control	1.32	1.35	1.39	1.44	1.50	1.57	1.63
Adjacent	1.32	1.34	1.37	1.41	1.46	1.50	1.53
Diagonally Adjacent	1.32	1.33	1.36	1.39	1.41	1.44	1.45

FWD = Fully Withdrawn

Table 4: Average Power Densities for Various 2 MW MNR Cores

Core	Total Fuel Meat Volume (cc)	Total BOL U-235 Mass (kg)	Total Power (MW)	Average Power Density in Fuel (W/cc)
48A	9265	4.746	2.00	216
48E	9265	4.661	2.00	216
48K	9456	4.704	2.00	212
48M	9341	4.664	2.00	214
49A	8807	4.626	2.00	227
49B	8807	4.700	2.00	227
49C	8807	4.749	2.00	227
49D	8807	4.860	2.00	227
48A – LEU	10180	5.472	2.00	196
49A – LEU	10180	5.466	2.00	196

Table 5: Maximum Calculated Radial Power-Peaking Factors (Core Site in Braces)

Core	PTR HEU 10-Plate	MNR HEU 18-plate	MNR LEU 225g U-235 18-Plate	MNR LEU 284g U-235 18-Plate	CTRL HEU 9-Plate	CTRL LEU 9-Plate
48A	2.04 (4D)	1.46 (3D)	-	1.06 (4F)	1.54 (4E)	-
48E	1.92 (4D)	1.47 (4C)	-	1.03 (4F)	1.51 (4E)	-
48K	2.00 (2D)	1.49 (4D)	-	1.00 (4F)	1.42 (4E)	-
48M	2.68 (4C)	1.49 (4D)	-	0.96 (4F)	1.38 (4E)	-
49A	2.31 (4C)	1.36 (4D)	0.71 (7E)	0.92 (4F)	1.45 (4B)	-
49B	2.28 (4C)	1.34 (4D)	1.20 (6C)	0.90 (4F)	1.42 (4B)	-
49C	2.25 (4C)	1.21 (4D)	1.50 (3C)	0.87 (4F)	1.44 (4B)	-
49D	1.92 (3E)	1.19 (3D)	1.64 (3C)	0.85 (4F)	1.42 (4B)	-
48A – LEU	-	-	1.50 (3D)	-	-	1.54 (4E)
49A – LEU	-	-	1.68 (4C)	-	-	1.52 (4B)
49A – 5 cm*	2.31 (4C)	1.36 (4D)	0.71 (7E)	0.92 (4F)	1.44 (4B)	-
49A – 10 cm*	2.31 (4C)	1.36 (4D)	0.71 (7E)	0.92 (4F)	1.42 (4B)	-
49A – 15 cm*	2.32 (4C)	1.37 (4D)	0.70 (7E)	0.92 (4F)	1.40 (4B)	-
49A – 20 cm*	2.32 (4C)	1.37 (4D)	0.70 (7E)	0.92 (4F)	1.37 (4B)	-
49A – 25 cm*	2.32 (4C)	1.37 (4D)	0.70 (7E)	0.92 (4F)	1.34 (4B)	-
49A – 30 cm*	2.32 (4C)	1.37 (4D)	0.70 (7E)	0.92 (4F)	1.31 (4B)	-

* Distance indicates absorber rod bank insertion, all other cases are for the absorbers in the fully withdrawn position

Table 6: Local, Axial, Radial, and Overall Power-Peaking Factors for the Various MNR Fuel Types

Fuel Type	Maximum Local Power-Peaking Factor	Maximum Radial Power-Peaking Factor	Maximum Axial Power-Peaking Factor	Maximum Overall Power-Peaking Factor
HEU 18-plate	1.39	1.49	1.53	3.17
HEU 10-plate	1.23	2.68	1.53	5.04
LEU 284g 18-plate	1.52	1.06	1.53	2.47
LEU 225g 18-plate	1.45	1.68	1.53	3.73
HEU Control	1.18	1.54	1.63	2.96
LEU Control	1.18	1.54	1.63	2.96

Table 7: Maximum Axially Averaged Power Ratings for the Various MNR Fuel Types at 2 MW

Fuel Type	Core 49A Average Power Density (W/cc)	Maximum Local Power-Peaking Factor	Maximum Radial Power-Peaking Factor	Hot Assembly Average Power Density (W/cc)	Fuel Meat Volume per Assembly (cc)	Hot Assembly Total Power Rating (kW)
HEU 18-plate	227	1.39	1.49	470	305	143
HEU 10-plate	227	1.23	2.68	748	191	143
LEU 284g 18-plate	227	1.52	1.06	366	305	112
LEU 225g 18-plate	227	1.45	1.68	553	305	169
HEU Control	227	1.18	1.54	413	172	71
LEU Control	227	1.18	1.54	413	172	71

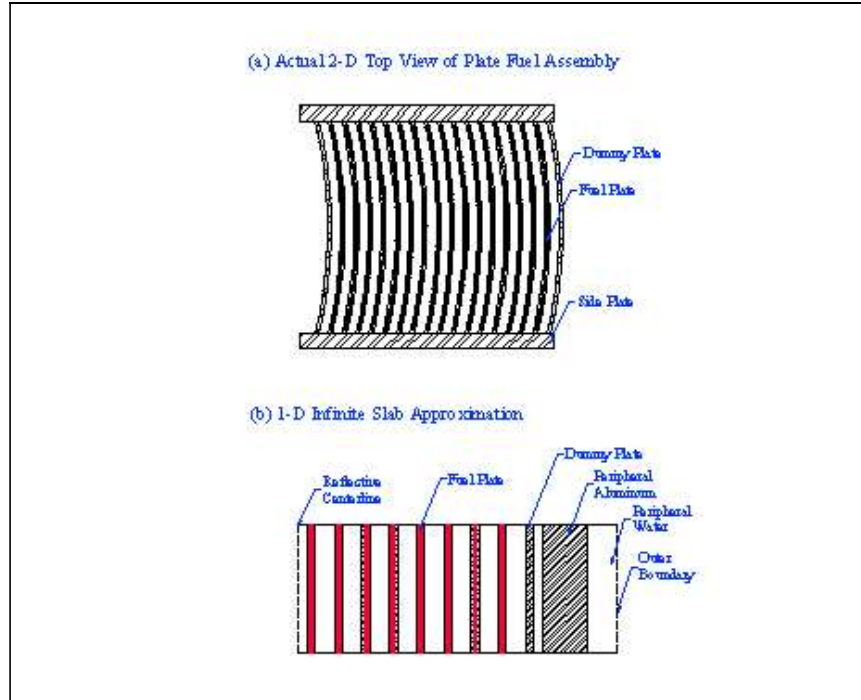


Figure 1: 1-D Infinite Slab Geometry Approximation for MNR Standard 18-Plate Fuel.

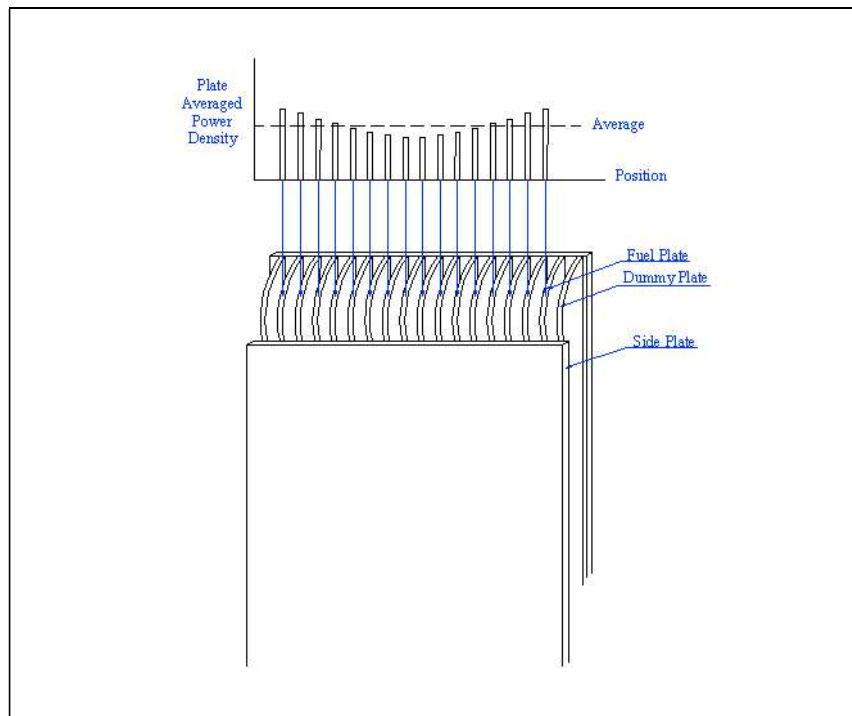


Figure 2: Schematic of the Local Power Density Distribution across a Plate Fuel Assembly.

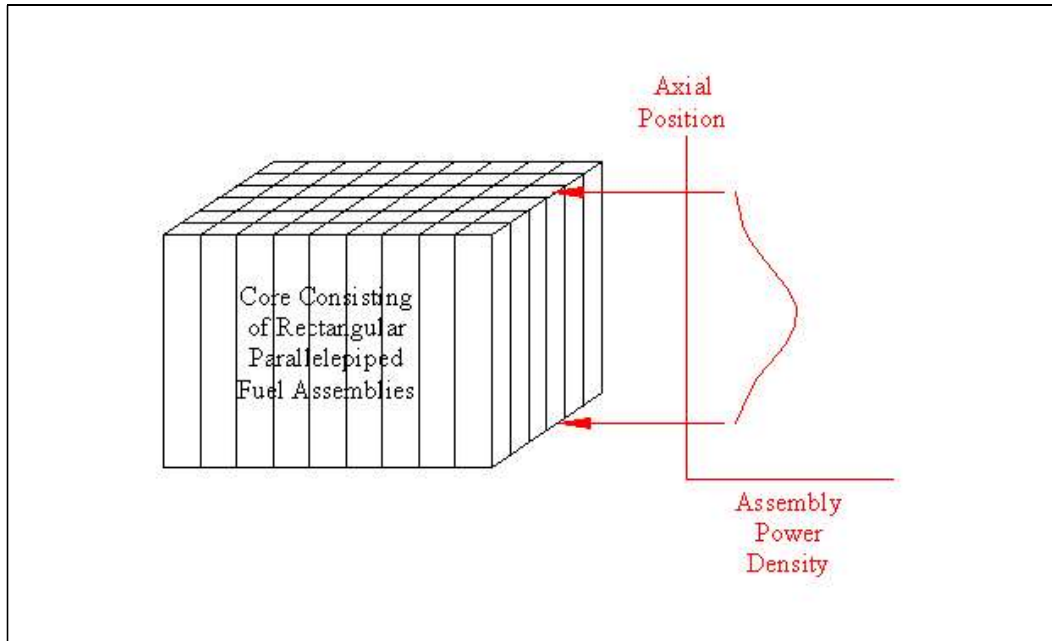


Figure 3: Schematic of Axial Power Peaking in the MNR Core.

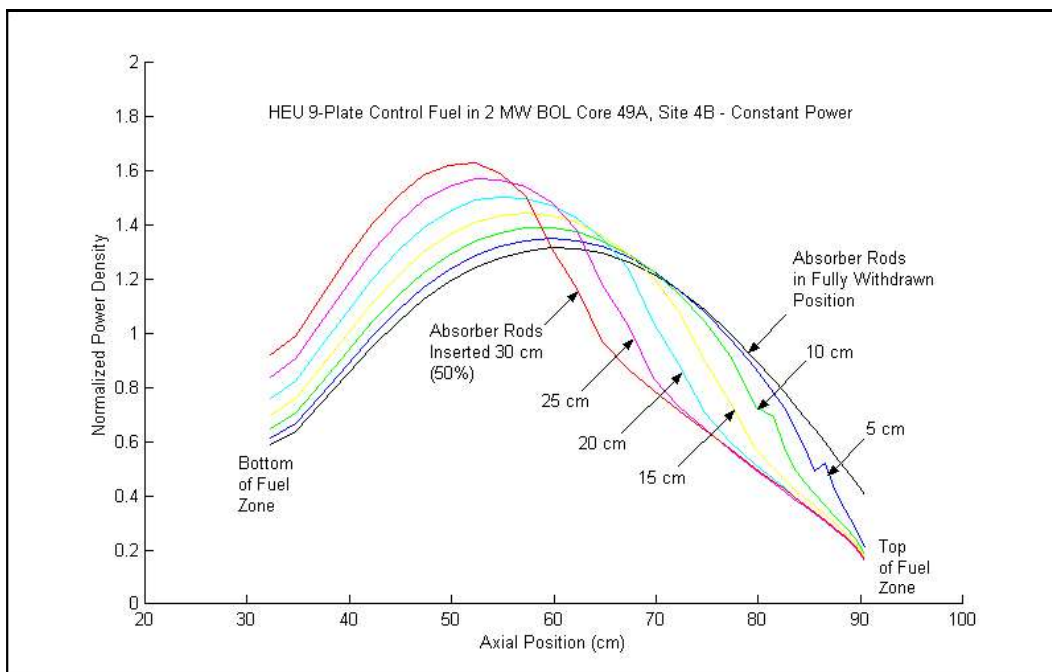


Figure 4: Axial Power Density Distribution for Various Absorber Rod Insertions at Constant Power (Note: Power Densities are Normalized to Average Assembly Power Density)

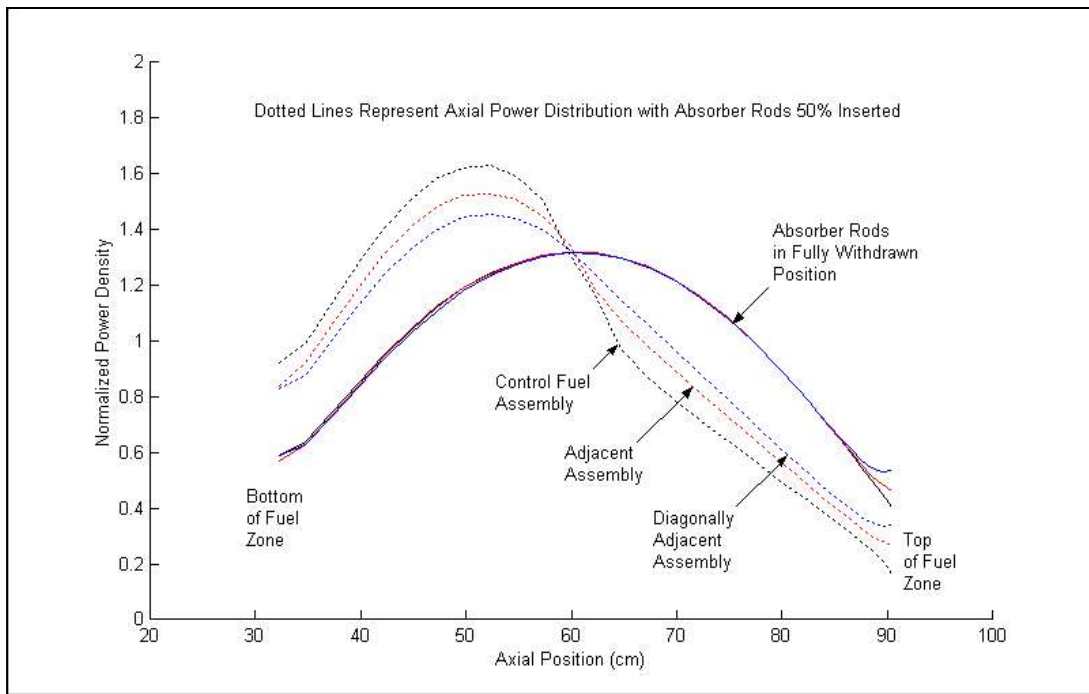


Figure 5: Axial Power Density Distribution for Various Fuel Assemblies in 2 MW Core 49A at Constant Power (Note: Power Densities are Normalized to Average Assembly Power Density)

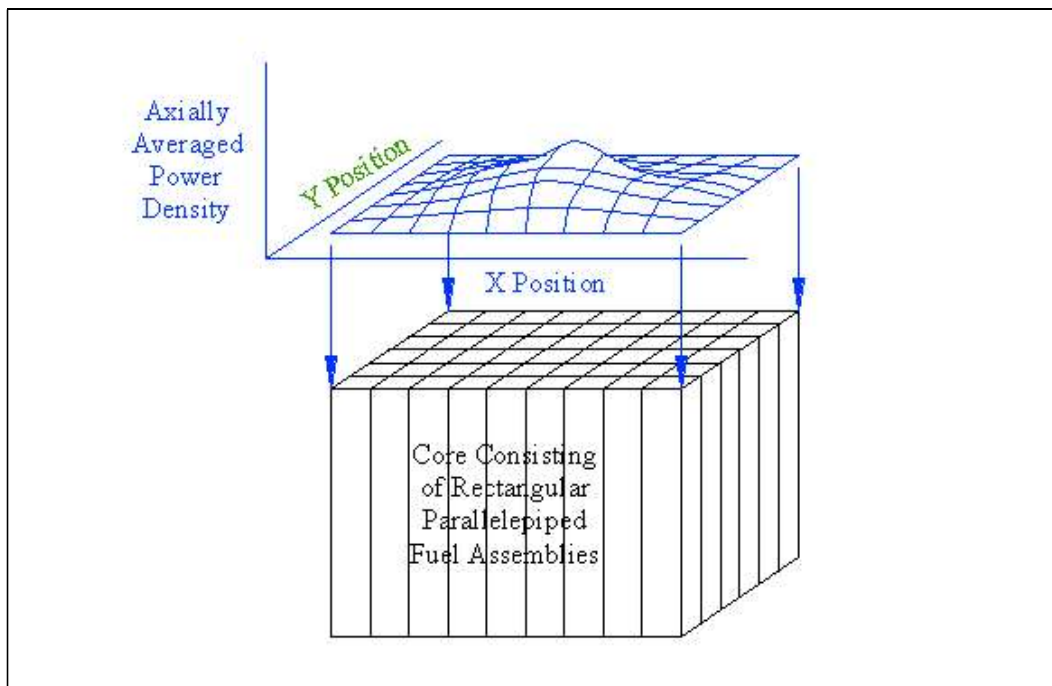


Figure 6: Schematic of Radial Power Peaking in the MNR Core.